



OPEN The secreted PAMP-induced peptide StPIP1_1 activates immune responses in potato

Linda Nietzsche¹, Ulrike Smolka¹, Elvio Henrique Benatto Perino¹, Karin Gorzolka¹, Gina Stamm², Sylvestre Marillonnet³, Katharina Bürstenbinder² & Sabine Rosahl¹✉

Treatment of potato plants with the pathogen-associated molecular pattern Pep-13 leads to the activation of more than 1200 genes. One of these, *StPIP1_1*, encodes a protein of 76 amino acids with sequence homology to PAMP-induced secreted peptides (PIPs) from *Arabidopsis thaliana*. Expression of *StPIP1_1* is also induced in response to infection with *Phytophthora infestans*, the causal agent of late blight disease. Apoplastic localization of *StPIP1_1*-mCherry fusion proteins is dependent on the presence of the predicted signal peptide. A synthetic peptide corresponding to the last 13 amino acids of *StPIP1_1* elicits the expression of the *StPIP1_1* gene itself, as well as that of pathogenesis related genes. The oxidative burst induced by exogenously applied *StPIP1_1* peptide in potato leaf disks is dependent on functional StSERK3A/B, suggesting that *StPIP1_1* perception occurs via a receptor complex involving the co-receptor StSERK3A/B. Moreover, *StPIP1_1* induces expression of *FRK1* in *Arabidopsis* in an RLK7-dependent manner. Expression of an RLK from potato with high sequence homology to AtRLK7 is induced by *StPIP1_1*, by Pep-13 and in response to infection with *P. infestans*. These observations are consistent with the hypothesis that, upon secretion, *StPIP1_1* acts as an endogenous peptide required for amplification of the defense response.

To defend themselves against pathogens, plants recognize not only pathogen-associated molecular patterns (PAMPs), but also structures derived from damage that has occurred during infection. Similar to PAMPs, these damage-associated molecular patterns (DAMPs) bind to plasma membrane-localized receptor kinases, leading to the activation of immune responses. DAMPs can be released passively upon cell disruption, as is the case for cell wall fragments and extracellular plant-derived compounds such as ATP¹, NAD(P)² and DNA³.

In contrast, there are endogenous danger signals that are actively processed and released into the apoplastic space. These include peptides that are produced from preproteins, such as systemin⁴, rapid alkalization factor RALF⁵, plant elicitor peptides (PEPs⁶), as well as the serine rich endogenous peptides (SCOOP⁷) and PAMP-induced peptides, PIPs⁸. These peptides, termed phytocytokines^{9–11}, are perceived by plasma membrane receptors^{8, 12–14}, thus activating immune responses such as cytosolic Ca²⁺ elevation, reactive oxygen species (ROS) burst, MAP kinase activation and transcriptional reprogramming^{8, 15, 16}.

The family of SGP-rich secreted endogenous peptides comprises not only the immunity-related PIPs and SCOOPs, but also Inflorescence Deficient in Abscission (IDA) peptides, which are involved in floral abscission¹⁷, thus emphasizing the dual role of phytocytokines in immunity and development. Apoplastic localization has been shown for *Arabidopsis* AtPIP1⁸, SCOOP10¹⁸ and IDA-like7 (IDL¹⁹), where they are postulated to bind to their respective receptors RLK7⁸, MIK2²⁰ and HAESA (HAE)/HAESA-LIKE2 (HSL2¹⁷).

In *Arabidopsis*, PIPs are encoded by 11 genes. Similar to PEP1²¹, AtPIP1 induces stomatal closure²², suggesting a role in stomatal immunity. Recently, the PAMP-induced peptides StPIP1 to StPIP4 were described in potato (*Solanum tuberosum*²³). Although exogenous application of chemically synthesized StPIP1 to leaves does not induce increases in the cytosolic Ca²⁺ concentrations nor ROS production, transgenic potato plants overexpressing StPIP1 show enhanced defense gene expression upon virus infection, suggesting a role of StPIP in eliciting defense responses²³.

One of the most devastating diseases of potato (*Solanum tuberosum*) is late blight, caused by the hemibiotrophic oomycete *Phytophthora infestans*. Treatment of susceptible plants with the PAMP Pep-13, a 13 amino acid oligopeptide from an extracellular transglutaminase from *Phytophthora* species, results in the activation

¹Department Biochemistry of Plant Interactions, Leibniz Institute of Plant Biochemistry, Weinberg 3, 06120 Halle (Saale), Germany. ²Department Molecular Signal Processing, Leibniz Institute of Plant Biochemistry, Weinberg 3, 06120 Halle (Saale), Germany. ³Department of Cell and Metabolic Biology, Leibniz Institute of Plant Biochemistry, Weinberg 3, 06120 Halle (Saale), Germany. ✉email: srosahl@ipb-halle.de

of salicylic acid and jasmonic acid-dependent immune responses, such as an oxidative burst, defense gene activation and hypersensitive cell death^{24–26}. Perception of Pep-13 requires the co-receptor BRI1-ASSOCIATED RECEPTOR KINASE1 (BAK1), encoded by two genes in potato, the SOMATIC EMBRYOGENESIS RECEPTOR KINASEs *StSERK3A* and *StSERK3B*²⁷. Transgenic potato plants with down-regulated expression of *StSERK3A/B* are unable to mount an oxidative burst or to activate MAP kinases in response to Pep-13 treatment²⁷.

We identified two novel *PIP1* genes in transcriptome analyses of Pep-13 activated genes. The two genes, *StPIP1_1* and *StPIP1_2*, encode the potato homologues of AtPIP1, whose secretion into the apoplast requires a signal peptide. Synthetic peptides encompassing the C-terminal 13 amino acids of *StPIP1_1* induce an oxidative burst in a *StSERK3A/B*-dependent manner and activate defense gene expression in potato leaves.

Results

StPIP1_1 and *StPIP1_2* are Pep-13-activated genes

StPIP1_1 and *StPIP1_2* were identified in microarray analyses as two of more than 1200 Pep-13-activated genes^{28, 29}. Specifically, transcript abundance of PGSC0003DMG400014649 (*StPIP1_1*) and PGSC0003DMG400006400 (*StPIP1_2*), predicted to encode 76 and 75 amino acid proteins, respectively, was enhanced in potato leaves after Pep-13 infiltration, compared to infiltration of the nearly inactive analogue W2A (Fig. S1A–C). In addition to the predicted signal peptide (LocTree3; Fig. 1A), the two encoded proteins contain a variable region and a highly conserved C-terminal region spanning 13 amino acids (Fig. 1A). Eleven of the C-terminal 13 amino acids of *StPIP1_1* (RLPSGSPRGPGRGH) are identical to those of AtPIP1 (RLASGSPRGRGH), whereas 10 out of 13 are identical in *StPIP1_2* (Fig. 1B, left panel). Sequence comparison also reveals that the recently identified *StPIP1* to *StPIP4*²³ have higher sequence homology to AtPIP2 (Fig. 1B, right panel). Due to the high sequence homology to AtPIP1, *StPIP1_1* was analyzed further. To gain insight into the temporal patterns of *StPIP1_1* induction in response to Pep-13 infiltration, *StPIP1* transcript levels were analyzed by qRT-PCR in time-course experiments (Fig. 1C). Phytochamber-grown potato plants were infiltrated with Pep-13 or the inactive analog W2A²⁴. Expression of *StPIP1_1* was significantly increased by Pep-13 treatment after 4 h and remained enhanced, compared to W2A treatment, until the end of the experiment at 24 h. Additional transcriptome analyses revealed that *StPIP1_1* also responded to infection by *P. infestans*, as did *StPIP1_2* and *StPIP1-4* (Fig. S2). Time-course experiments showed that *StPIP1_1* transcript levels were significantly increased 2 and 3 days after inoculation with *P. infestans* (Fig. 1D). Thus, both PAMP-treatment and infection by *P. infestans* induced *StPIP1_1* gene expression.

StPIP1_1 activates immune responses

The C-terminal 13 amino acids of AtPIP1 were described to activate defense gene expression⁸. We therefore assessed the elicitor activity of a synthetic oligopeptide covering the respective C-terminal 13 amino acids of *StPIP1_1* (Fig. 1B). Infiltration of this peptide into potato leaves resulted in enhanced *StPIP1_1* transcript levels starting 4 h after treatment (Fig. 2A). Moreover, expression of *StPR1* encoding the sterol binding protein *PATHOGENESIS-RELATED 1*³⁰, *St4CL* (*4-COUMARATE-COA-LIGASE*) and *StTHT* (*TYRAMINE HYDROXYCINNAMOYL-COA TRANSFERASE*³¹) was enhanced in response to *StPIP1_1* (Fig. 2B–D).

To test if altered defense-gene expression correlates with metabolic changes in *StPIP1_1* treated plants, we determined the accumulation of specialized metabolites using untargeted metabolite profiling by UPLC-ESI-QTOF-MS of methanolic leaf extracts. Sixty-seven features were at least twofold higher in plants treated with *StPIP1_1* for 8 h compared to water-treated plants or plants treated with *StPIP1_1* for 1 h. In accordance with increased transcript levels of *4-CL* and *THT*, which encode enzymes involved in the synthesis of hydroxycinnamic acid amides, we identified the defense metabolites *p*-coumaroyl- and feruloyloctopamine (Fig. 2E,F) as well as *p*-coumaroyltyramine³² (Fig. 2G) as *StPIP1_1*-induced compounds. Feruloyltyramine, on the other hand, was less than twofold enhanced after 8 h (Fig. 2H). Thus, *StPIP1_1* induced defense gene expression and accumulation of defense metabolites suggesting that perception of *StPIP1_1* leads to the activation of several defense-related traits.

StPIP1_1-mCherry is secreted into the apoplast

StPIP1_1 and *StPIP1_2* contain predicted signal peptides at their N-terminus suggesting that the proteins are targeted to the secretory pathway for apoplastic delivery. The localization of *StPIP1_1* was determined by transient expression of a C-terminally mCherry tagged protein expressed under control of the CaMV 35S promoter in *Nicotiana benthamiana* (*StPIP1_1*-mCh). The coding region of *StPIP1_1* was cloned in front of an intron-containing mCherry gene to ensure that mCherry signals are derived from plant-expressed transcripts. To address the importance of the signal peptide, we included a variant lacking the first 87 nucleotides, encoding the predicted signal peptide of 29 amino acids (Δ SP-*StPIP1_1*-mCh). As plasma membrane marker, Arabidopsis sulfate transporter SULTR1;2-GFP was co-expressed³³. Confocal microscopy imaging revealed localization of *StPIP1_1*-mCherry fluorescence in the apoplastic space that lies between GFP-SULTR1;2-GFP labeled plasma membranes (Fig. 3A). Apoplastic localization was validated in cells plasmolyzed upon treatment with 150 mM NaCl (Fig. 3B), which confirmed *StPIP1_1*-mCherry accumulation in the extracellular space between cell walls and the plasma membrane. The variant lacking the predicted signal peptide, Δ SP-*StPIP1_1*-mCh displayed cytosolic and nuclear localization (Fig. 3C,D). Western blot analysis demonstrated expression of full-length *StPIP1_1*-mCh and Δ SP-*StPIP1_1*-mCh (Fig. 3E, Fig. S3). In addition, bands of smaller molecular weight were detected in samples from cells expressing *StPIP1_1*-mCh. The smaller variants may result from extracellular proteolytic cleavage of *StPIP1_1*-mCh or may represent partially or fully processed *StPIP1_1* pre-protein or the active *StPIP1_1* peptide. Our analysis thus demonstrates that *StPIP1_1* contains a functional signal peptide and is secreted to the apoplast via the secretory way where it is predicted to function as PAMP-induced peptide during plant defense responses.

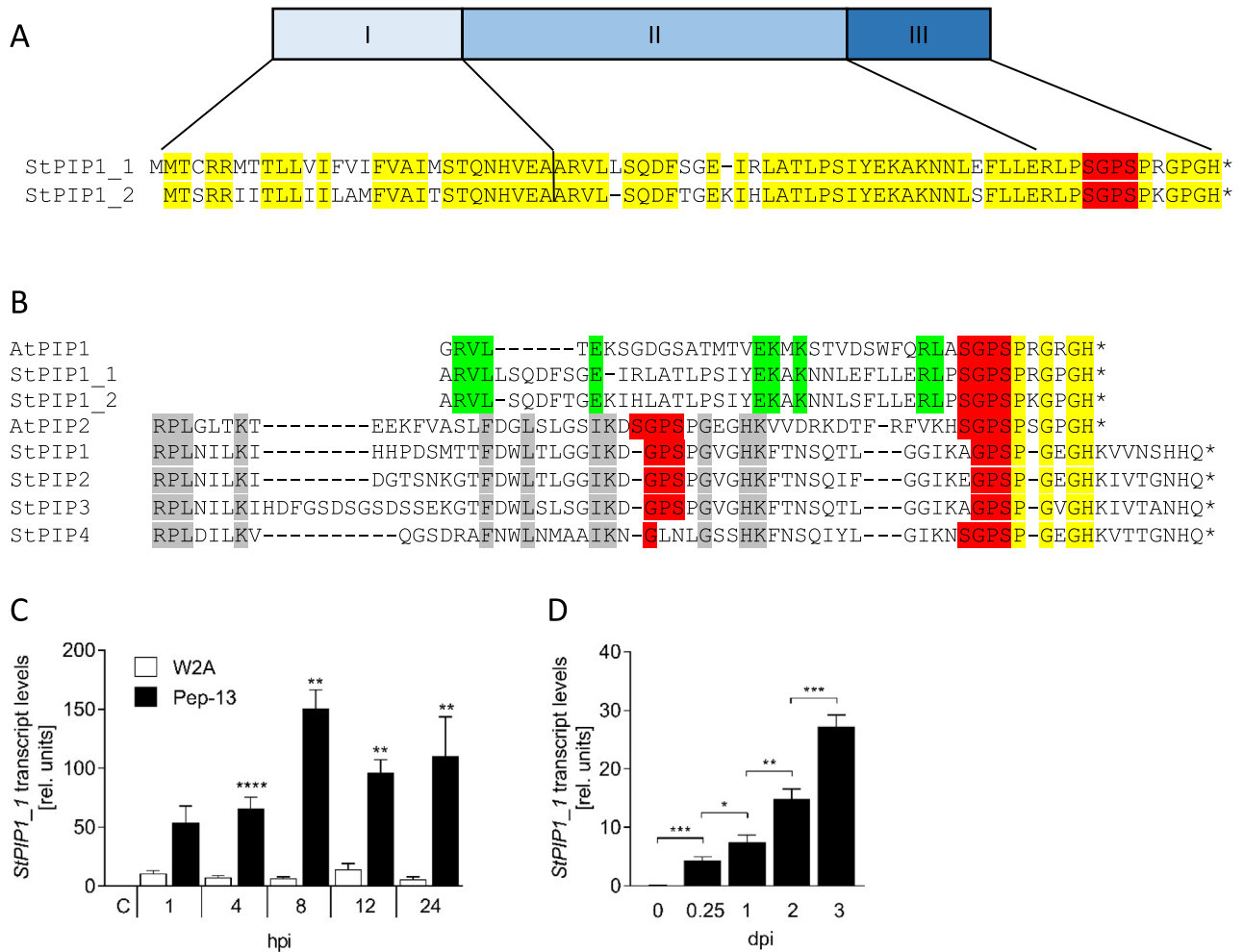


Figure 1. Structure of StPIP1_1 and expression in response to Pep-13 treatment and *P. infestans* infection. (A) Domain structure of StPIP1_1 and StPIP1-2. Domain I: signal peptide, domain II: variable region, domain III: conserved region. Conserved amino acids conserved are marked in yellow. The SGPS motif is marked in red. (B) Amino acid sequence of the predicted mature proteins AtPIP1 and AtPIP2 with those of potato StPIP1_1 and StPIP1_2, as well as StPIP1, 2, 3 and 4 (Combest et al.²³). Amino acids conserved between AtPIP1 and StPIP1_1 and StPIP1_2 are marked in green, those conserved between AtPIP2 and StPIP1 to StPIP4 in grey and those conserved in all proteins in yellow. The SGPS and GPS motifs are marked in red. (C) *StPIP1_1* transcript accumulation in response to Pep-13. RNA was isolated from W2A (white bars) or Pep-13 (black bars) infiltrated potato leaves at the time points indicated (hours post infiltration, hpi) and subjected to qRT-PCR analyses. Data shown were normalized to the expression of *StEF1a* and are derived from three independent experiments ($n \geq 6$, except for 1 hpi Pep-13: $n = 5$). Error bars represent SEM. Statistical differences between W2A and Pep-13-infiltrated plants were determined by Mann Whitney U test (** $p \leq 0.001$; **** $p \leq 0.0001$). (D) *StPIP1_1* transcript accumulation in response to *P. infestans* infection. RNA was isolated from *P. infestans*-inoculated potato leaves at the time points indicated (days post inoculation, dpi) and subjected to qRT-PCR analyses. Data shown were normalized to the expression of *StEF1a* and are derived from three independent experiments ($n = 8$). Error bars represent SEM. Statistical analyses were performed by Mann Whitney U test (* $p \leq 0.05$; ** $p \leq 0.01$; *** $p \leq 0.005$).

StPIP1_1 induces an oxidative burst in a SERK3A/B-dependent manner

One of the early responses to pathogen attack or PAMP/DAMP treatment is the oxidative burst. The oligopeptide StPIP1_1 was analyzed for its ability to induce the generation of ROS when added to leaf disks of potato plants. In contrast to water treatment, incubation with StPIP1_1 induced significantly enhanced levels of ROS (Fig. 4A). Since the leucine-rich receptor-like kinase BAK1 is part of the receptor complex required for perception of several peptides in Arabidopsis³⁴, we addressed the importance of the co-receptor BAK1 for StPIP1_1-induced ROS formation. The oligopeptide was added to leaf disks of transgenic plants expressing an RNA interference construct against the two genes in potato, which encode the BAK1 isoforms *StSERK3A* and *StSERK3B*²⁷. In these plants, StPIP1_1 was unable to induce an oxidative burst (Fig. 4B), suggesting a requirement for BAK1 as a co-receptor for StPIP1_1 perception.

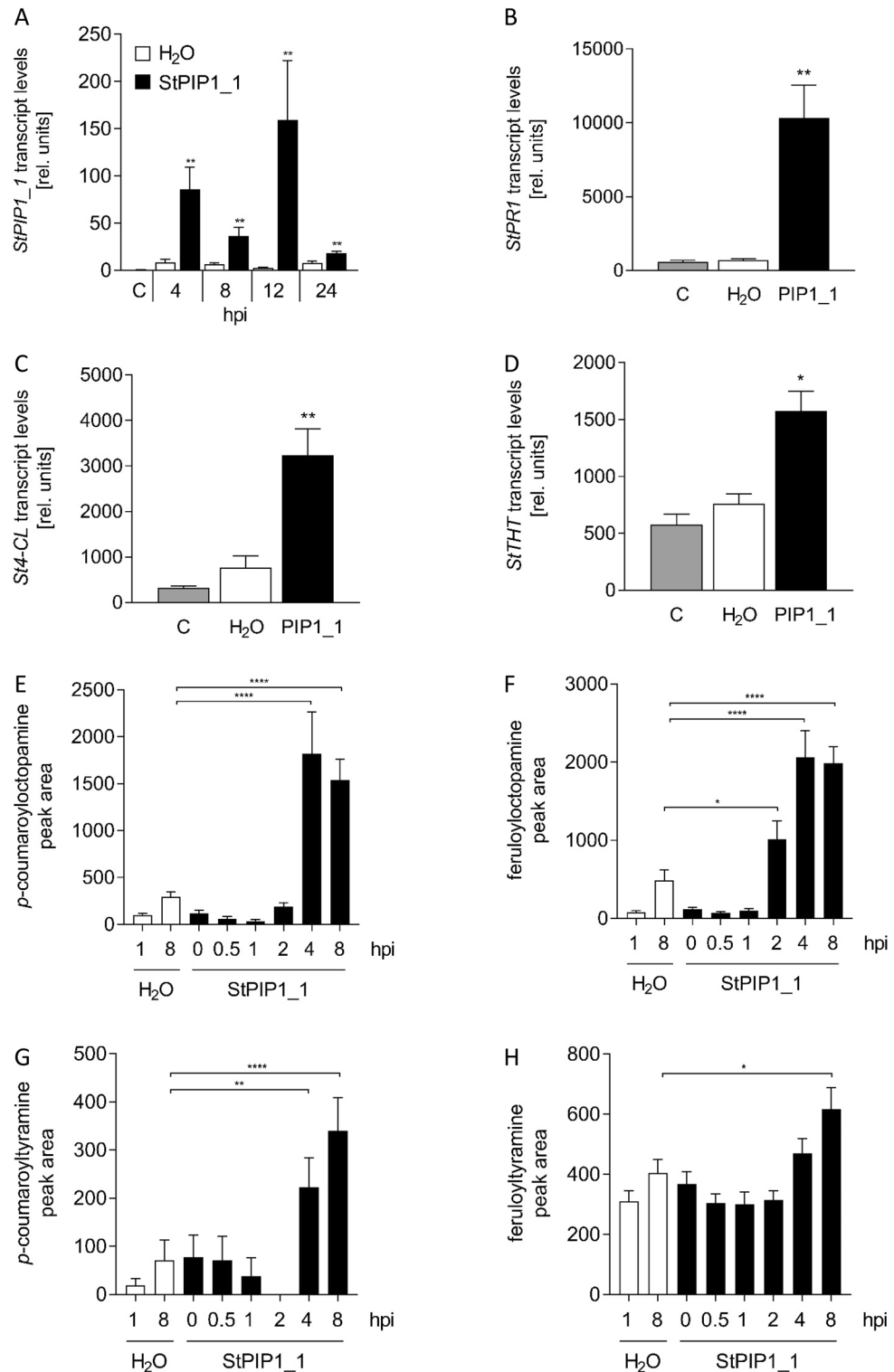


Figure 2. StPIP1_1 induces defense gene expression and accumulation of defense metabolites. (A–D) RNA was isolated from untreated (“C”, grey bar), water-treated (white bars) or StPIP1_1 (black bars) infiltrated potato leaves and subjected to qRT-PCR analyses. Data shown were normalized to the expression of *StEF1α* and are derived from two independent experiments. Error bars represent SEM. Statistical differences between water-treated and StPIP1_1-treated plants were determined by Mann Whitney U test (* $p \leq 0.05$; ** $p \leq 0.001$). (A) *StPIP1_1* transcript levels after infiltration of StPIP1_1 at the time points indicated. $n = 6$. (B) *StPR1* transcript levels 4 h after infiltration of StPIP1_1. $n \geq 6$. (C) *St4CL* transcript levels 4 h after infiltration of StPIP1_1. $n = 5$. (D) *StTHT* transcript levels 4 h after infiltration of StPIP1_1. $n = 5$. (E–H) Metabolite profiling was performed on methanolic extracts from potato leaves infiltrated with water or StPIP1_1 for the time points indicated (hours post infiltration). (E) *p*-coumaroyltyramine, (F) feruloyltyramine, (G) *p*-coumaroyloctopamine, (H) feruloyloctopamine. Data are derived from two independent experiments ($n \geq 17$). Error bars represent SEM. Statistical differences were determined by Mann Whitney U test (* $p \leq 0.05$; ** $p \leq 0.01$; **** $p \leq 0.001$).

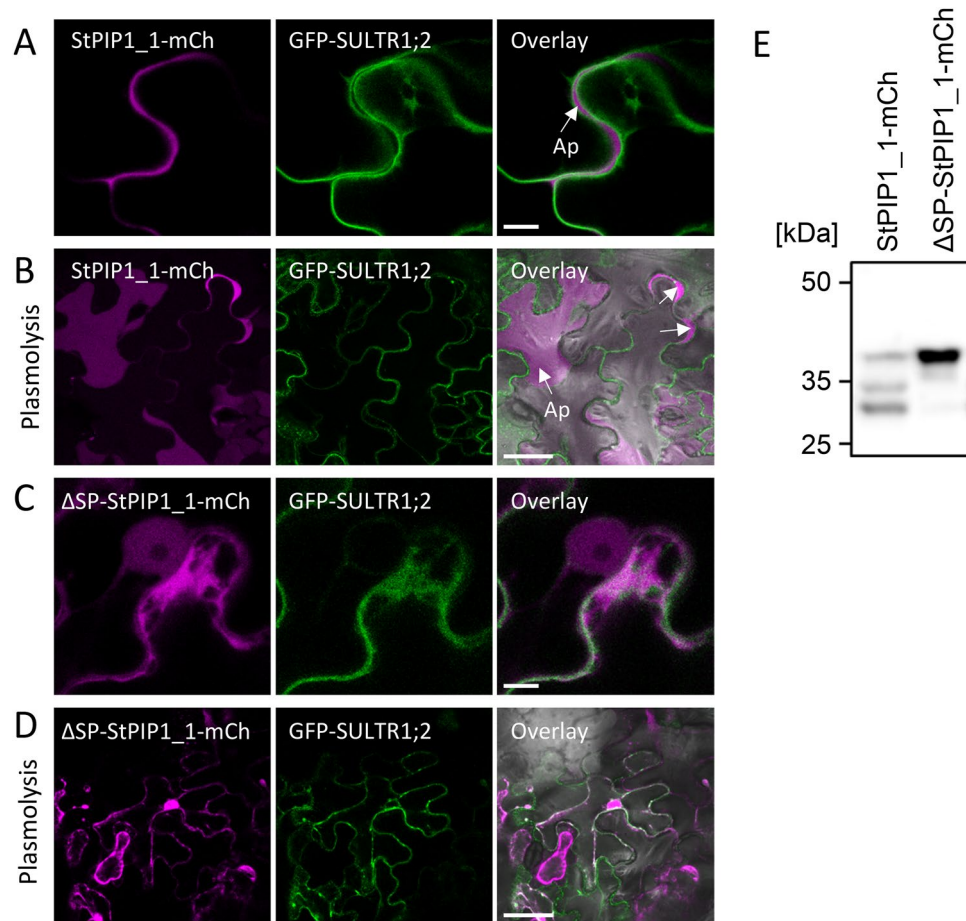


Figure 3. StPIP1_1 is exported into the apoplast. The coding region of StPIP1_1, or the coding region without the predicted signal peptide (ΔSP_StPIP1_1) fused to intron-containing mCherry (StPIP1_1-mCh and ΔSP_StPIP1_1-mCh) under the control of the 35S promoter, were transiently expressed in *N. benthamiana*, together with the GFP-tagged plasmamembrane protein SULTR1;2. **(A)** GFP, mCherry and merged fluorescence of SULTR1;2-GFP and StPIP1_1-mCh. Scale bars represent 10 μm. **(B)** Plasmolysis of *N. benthamiana* leaves after transient expression of StPIP1_1-mCh and SULTR1;2-GFP was induced by 150 mM NaCl. GFP, mCherry and merged fluorescence is shown. Scale bars represent 50 μm. **(C)** GFP, mCherry and merged fluorescence of SULTR1;2-GFP and ΔSP_StPIP1_1-mCh (without signal peptide). Scale bars represent 10 μm. **(D)** Plasmolysis in *N. benthamiana* leaves after transient expression of ΔSP_StPIP1_1-mCh and SULTR1;2-GFP was induced by 150 mM NaCl. GFP, mCherry and merged fluorescence is shown. Scale bars represent 50 μm. **(E)** Transient expression of fusion proteins in *N. benthamiana*. Proteins were extracted from *N. benthamiana* leaves expressing StPIP1_1-mCh or ΔSP_StPIP1_1-mCh 3 days after *Agrobacterium* infiltration and subjected to Western blot analyses using an α-RFP antibody.

StPIP1_1 induces *FRK* gene expression in Arabidopsis in an RLK7-dependent manner

Arabidopsis PIP1 has been described to bind to the receptor-like kinase (RLK) 7 and to activate defense responses⁸. To address whether StPIP1_1 is able to act in a similar manner, seedlings of the Arabidopsis wild type Col-0 and of the *rlk7-2* knock out mutant were treated with the oligopeptide StPIP1_1. As a control, AtPIP1 was included and the two peptides were analyzed for their ability to induce the expression of *FLG22-INDUCED RECEPTOR-LIKE KINASE 1 (FRK1)*. Consistent with published data, transcripts of *FRK1* accumulated in response to AtPIP1⁸. Interestingly, application of StPIP1_1 induced *FRK1* expression to a similar level (Fig. 5A). In the *rlk7-2* mutant, *FRK1* expression was not induced by neither AtPIP1 nor StPIP1_1, indicating that StPIP1_1 acts as a functional homolog of AtPIP1. This observation moreover suggests that StPIP1_1 might bind to an RLK7 homolog from potato. Comparing the amino acid sequence of RLK7 with the potato database, two putative RLKs were identified with 62 and 56% identity to RLK7 from Arabidopsis. Transcripts of RLK7-like 1 (StR7L1; PGSC0003DMG400004966) did not accumulate in response to Pep-13 treatment in infiltrated potato leaves, while RLK7-like 2 (StR7L2; PGSC0003DMG400005103) transcript levels were elevated (Fig. S4). To verify this expression, independent experiments were carried out. Pep-13 induced transcript accumulation of StR7L2 already 1 h after infiltration (Fig. 5B), and in response to StPIP1_1, significantly higher levels compared to untreated plants were observed after 4 h (Fig. 5C). Moreover, *P. infestans* infection led to enhanced levels of StR7L2 transcripts starting 1 day after inoculation, remaining high until the end of the experiment at 3 days

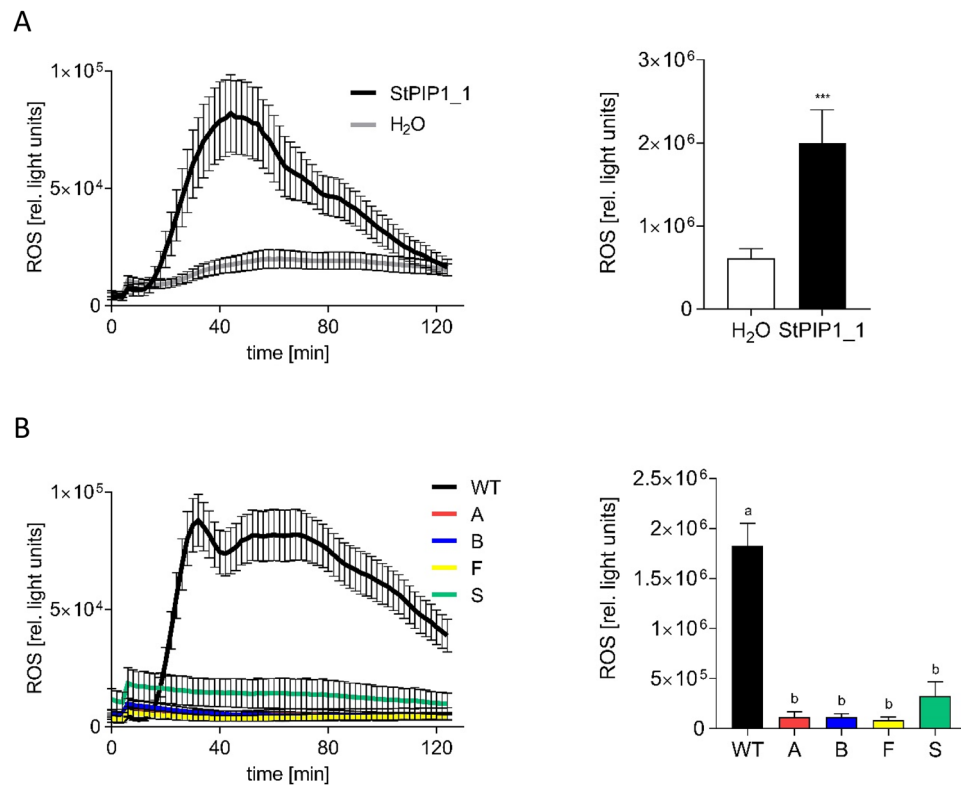


Figure 4. StPIP1_1 induces an oxidative burst in potato leaf disks in a StSERK3A/B-dependent manner. Leaf disks of phytochamber-grown potato plants were incubated with 100 nM StPIP1_1 and assayed for luminol-based ROS production. **(A)** ROS formation in leaf disks of wild type plants in response to StPIP1_1 (black) or water (grey). To quantify the ROS burst, light units up to 80 min were added (right panel). Error bars represent SEM. Data are derived from two independent experiments ($n \geq 24$). Statistical analyses were performed using Mann Whitney U test ($***p \leq 0.01$). **(B)** ROS formation in leaf disks of wild type (WT, black) and four independent StSERK3A/B-plants (A: red, B: blue, F: yellow, S: green) in response to StPIP1_1. To quantify the ROS burst, light units up to 80 min were added (right panel). Error bars represent SEM. Data are derived from two independent experiments (WT: $n = 40$, A,B,F,S: $n = 24$). Statistical analyses were performed using One-way-Anova. Different letters indicate significant differences.

(Fig. 5D). Thus, both StPIP1_1 and StR7L2 were responsive to the PAMP Pep-13, the phyto cytokine StPIP1_1 and to infection by *P. infestans*.

StPIP1_1 and Pep-13 are rapidly degraded upon infiltration into potato leaves

Exogenous application of peptides is routinely used to address their ability to activate immune responses, however, little is known about stability of peptides in plants. Our metabolomics analyses allowed the detection of exogenously applied peptides and their degradation products. We therefore screened the metabolomics data for StPIP1_1 peptides. When applied as an amide, StPIP1_1 was rapidly degraded to 20 and 10% within 30 min and 1 h, respectively (Fig. 6A). Interestingly, the deaminated acidic form of StPIP1_1 was detected within minutes. Two hours after infiltration, 30% of the initial amount was still present, decreasing to 13 and 5% after 4 and 8 h, respectively (Fig. 6B). This suggests that, upon infiltration, the amidated peptide was rapidly and efficiently converted to the acidic form, which, in turn, was degraded within 4 h. To analyze whether this effect is specific for StPIP1_1, we performed an equivalent experiment with Pep-13, the PAMP from *Phytophthora* species. As StPIP1_1, the amidated peptide was converted to the acidic form within 30 min (Fig. 6C), which was also degraded within 1 h (Fig. 6D). These results indicate that exogenously applied peptides do not persist in the apoplast, but are rapidly metabolized.

Our study shows that the potato homolog of AtPIP1 is secreted to the apoplast in a signal peptide-dependent manner, that the induction of early defense responses is dependent on BAK1 and that StPIP1_1 activates immune responses, including its own expression.

Discussion

StPIP1_1 is a functional homolog of AtPIP1

The potato genome contains genes encoding small secreted proteins which are induced by PAMP treatment or pathogen infection. Combest et al.²³ reported that transcripts encoding the peptides StPIP1 to StPIP4 accumulate

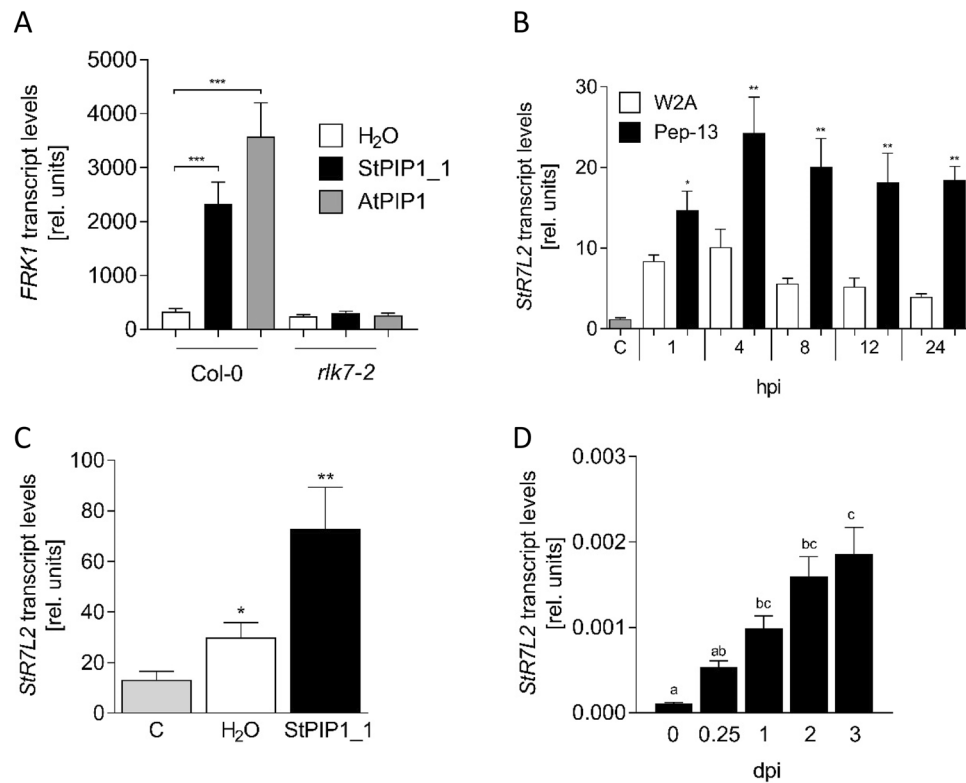


Figure 5. RLK7-dependent StPIP1_1-induced gene expression in Arabidopsis and expression of a potato gene encoding an LRR-RLK with sequence homology to RLK7. **(A)** StPIP1_1 from *S. tuberosum* induces *FRK1* transcript accumulation in a RLK7-dependent manner. Arabidopsis seedlings (Col-0 and the T-DNA insertion mutant *rlk7-2* (SALK_083114)) were treated with water (C, white bar), 1 μ M StPIP1_1 (black bars) or AtPIP1 (grey bars). RNA was isolated after 4 h and subjected to qRT-PCR. Data are derived from three independent experiments ($n=7$). Error bars represent SEM. Statistical analyses were performed using One-way-Anova. Different letters indicate statistically different values. **(B)** PAMP-induced expression of the LRR-RLK gene *StR7L2* with sequence homology to RLK7. RNA was isolated from untreated (C, grey bar), W2A (white bars) and Pep-13 (black bars) infiltrated potato leaves and subjected to qRT-PCR analyses. Expression was normalized to that of *StEF1 α* . Data are derived from three independent experiments ($n \geq 5$). Error bars represent SEM. Statistical analyses were performed using Mann Whitney U test ($*p \leq 0.05$, $**p \leq 0.001$) and show differences between W2A- and Pep-13-infiltrated plants. **(C)** StPIP1_1-induced expression of *StR7L2*. RNA was isolated from untreated leaves (“C”, grey bar) or 4 h after infiltration of water (white bars) or StPIP1_1- (black bars) and subjected to qRT-PCR analyses. Data shown were normalized to the expression of *StEF1 α* and are derived from two independent experiments ($n \geq 11$). Error bars represent SEM. Statistical differences between control plants and water-treated or StPIP1_1-treated plants were determined by Mann Whitney U test ($*p \leq 0.05$; $**p \leq 0.001$). **(D)** *P. infestans*-induced expression of *StR7L2*. RNA was isolated from *P. infestans*-infected leaves at the time points indicated and subjected to qRT-PCR analyses. Data shown were normalized to the expression of *StEF1 α* and are derived from two independent experiments ($n=8$). Error bars represent SEM. Different letters represent significant differences as determined by One-way-Anova.

in response to infection with potato virus Y. These peptides show highest sequence homology to the Arabidopsis peptide AtPIP2²³ (Fig. 1), which contains two GPS motifs. In contrast, the potato PIPs described here, StPIP1_1 and StPIP1_2, are more similar to AtPIP1 and only harbor a C-terminal SGPS motif. Combest et al.²³ used a peptide of 23 amino acids covering the C-terminal GPS motif of StPIP1 (TLGGIKAGPSPGEGHKVVNSHHQ) to analyze immune responses. This peptide has highest sequence homology to the first motif in AtPIP2 (15 identical amino acids out of 23), and less to the C-terminal motifs in AtPIP2 (9 out of 23) or AtPIP1 (7 out of 23). Hou et al.⁸ used a peptide comprising the last 13 amino acids of AtPIP1. StPIP1_1 and StPIP1_2 have 11 and 10 identical amino acids, respectively, out of these 13 amino acids comprising the SGPS motif of AtPIP1. Moreover, AtPIP1, AtPIP2 and the two PIPs identified in our study represent the C-terminal amino acids, whereas StPIP1-4 have additional amino acids downstream of the GPS motif. Thus, we conclude that StPIP1_1 identified in this study is the potato PIP family member with the highest amino acid sequence homology to AtPIP1.

Similar to AtPIP1, exogenous application of a synthetic peptide covering the C-terminal 13 amino acids of StPIP1_1 to Arabidopsis seedlings induces *FRK1* expression. Importantly, this induction does not take place in a mutant defective in *RLK7*, encoding the receptor-like kinase that binds AtPIP1⁸, suggesting that StPIP1_1 is a functional homolog of AtPIP1.

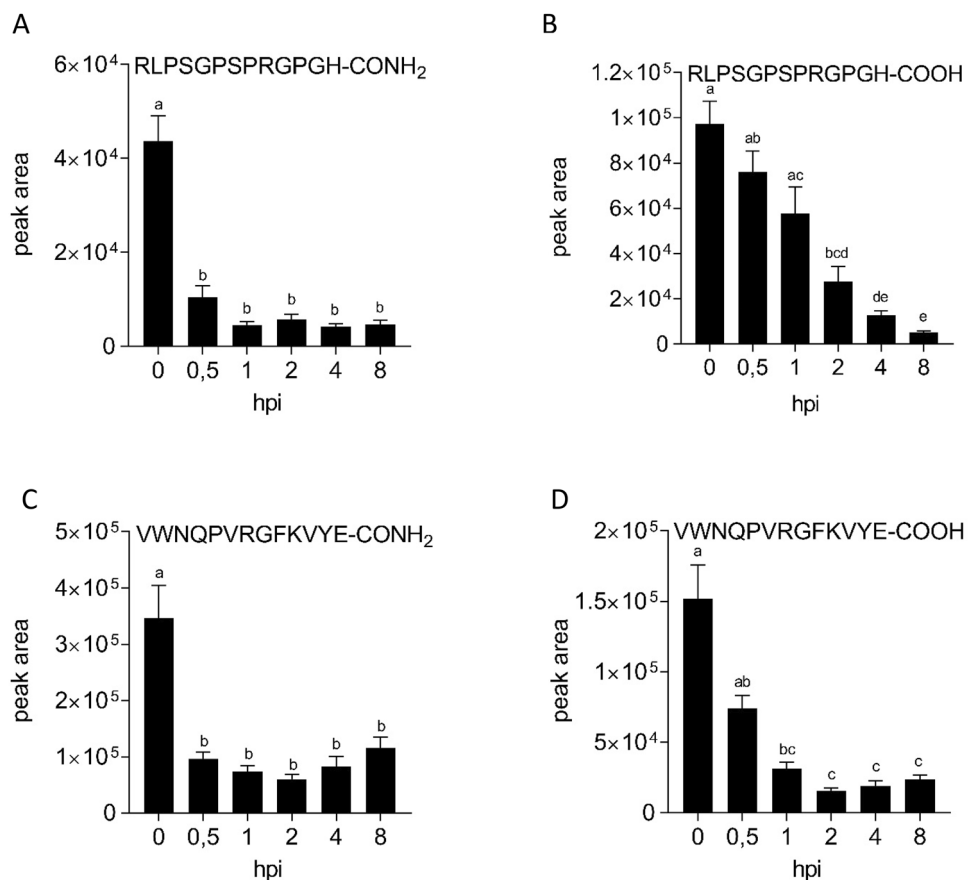


Figure 6. Peptides are rapidly degraded after infiltration into potato leaves. Phytochamber-grown potato plants were infiltrated with 100 μ M amidated StPIP1_1 (A,B) or Pep-13 (C,D). Leaf samples were taken at the time points indicated and subjected to LC–MS analyses to determine the levels of amidated (A,C) and deaminated (B,D) peptides. Data are derived from two independent experiments ($n = 16$, except time point 0 in C and D: $n = 12$). Error bars represent SEM. Statistical analyses were performed using One-way-Anova. Different letters represent significant differences.

StPIP1_1 induces immune responses in leaves

In response to treatment with StPIP1_1, we observed significant ROS production in potato leaf disks. In contrast, Combest et al.²³ reported a ROS burst induced by StPIP1 only in nodes, but not in leaves. On the other hand, both StPIP1 and StPIP1_1 induced defense gene expression. In addition, we showed that defense metabolites, such as *p*-coumaroyl- and feruloyloctopamine, as well as *p*-coumaroyltyramine, accumulated in StPIP1_1-infiltrated plants. In potato, these compounds are synthesized in response to pathogen infection or PAMP treatment³². They are incorporated into the cell wall and are therefore postulated to contribute to pathogen resistance³¹. Indeed, overexpression of the tomato gene encoding the biosynthetic enzyme THT in transgenic plants resulted in enhanced levels of HCAAs and correlated with reduced growth of *Pseudomonas syringae* pv. *tomato*³⁵.

The StPIP1_1-induced production of ROS and the accumulation of defense transcripts and metabolites in potato leaves suggest that StPIP1_1 indeed acts as a phyto cytokine. In transgenic plants overexpressing StPIP1, no difference in gene expression to wild type plants was observed²³. However, inoculation with potato virus Y resulted in the activation of a large number of genes in StPIP1 overexpressing plants, compared to the lower number of genes induced by PVY in control plants²³, suggesting that StPIP1, once induced, amplifies the defense response. This is in accordance with Arabidopsis plants expressing AtPIP1, which displayed enhanced resistance to the root pathogen *Fusarium oxysporum*⁸.

A signal peptide is required for apoplastic localization of StPIP1_1

In order to act as a phyto cytokine, peptides have to be present in the apoplast. This can be achieved by secretion or by release into the apoplast after cellular damage. The proprotein of Arabidopsis AtPEP1 is released upon wounding and subsequently processed by Ca²⁺-dependent metacaspases³⁶. More specifically, the metacaspase MC4 cleaves the precursor of PEP1 (PROPEP1) after a conserved arginine, resulting in the release of the C-terminal 23 amino acids that make up PEP1^{36,37}. In contrast, AtPIP1-GFP fusion proteins were present in the apoplast of non-disrupted cells after transient expression in *N. benthamiana* leaves⁸. Here we show that the apoplastic localization of potato StPIP1_1 is dependent on the presence of the predicted N-terminal signal peptide, suggesting

that potato StPIP is targeted to the extracellular compartment by the secretory pathway. Similarly, IDA, a peptide with sequence similarity to PIPs, was also shown to be secreted in a signal peptide-dependent manner³⁸.

Nicotiana benthamiana cells transiently expressing StPIP1_1-mCh contain proteins with a lower molecular weight than those expressing ΔSP_StPIP1_1-mCh, suggesting extracellular processing of the proprotein in the apoplast by yet unidentified proteases. In vitro experiments with GST-tagged AtPIP1 and AtPIP2, incubated with Arabidopsis protein extracts, also revealed processing of the proproteins, however, the proteases responsible or the nature of the released peptides had not been confirmed by proteomics⁸. For only a few apoplastic peptides, processing by proteases has been shown. The IDA peptide, for example, is released by subtilisin-like proteases³⁹, whereas the apoplastic immune signaling peptide ZIP1 from maize is released from its proprotein by the action of Papain-like cysteine proteases⁴⁰. In this context it is interesting to note that exogenously applied synthetic peptides are rapidly degraded, possibly by apoplastic proteases that are part of the immune barrier at the plant pathogen interface.

StPIP1_1 perception requires the co-receptor BAK1

ROS production induced in potato leaf disks by StPIP1_1 was dependent on the functional co-receptors StSERK3A/B, the potato homologs of BAK1 from Arabidopsis, since no hydrogen peroxide formation was detected in *StSERK3A/B* silenced plants. Loss of ROS production in *StSERK3A/B*-silenced plants had also been observed in response to Pep-13 and flg22, but not chitin, suggesting that *StSERK3A/B* are required for peptide perception²⁷. In Arabidopsis, the ROS burst induced by AtPIP1 was shown to be partially dependent on BAK1⁸. In addition, the induction of stomatal closure by AtPIP1 in Arabidopsis is also dependent on functional BAK1⁴¹. Thus, PIP peptides are suggested to be perceived by a receptor complex involving BAK1 in both Arabidopsis and potato. Data obtained in Arabidopsis moreover imply that such a receptor complex would include receptor kinase RLK7^(8, 22, 41). Since StPIP1_1 is a functional homolog of AtPIP1, we searched for a possible homolog of RLK7 in potato. Comparison of the amino acid sequence of RLK7 to the potato database revealed homology to StR7L1 and StR7L2. As reported by Combest et al.²³, transcripts of StR7L1 did not accumulate in virus-inoculated StPIP1 overexpressing plants, which is in accordance with our observation that expression is not induced after Pep-13 treatment. In contrast, transcripts of StR7L2 accumulate in response to PAMP treatment and pathogen infection. Thus, the encoded RLK is a candidate for the RLK7 homolog of potato.

Our data suggest that the potato homolog of AtPIP1, StPIP1_1, is secreted to the apoplast, causes an oxidative burst in a BAK1-dependent manner and induces defense gene expression as well as defense metabolite accumulation.

Methods

Plant culture and treatments

Potato plants (*Solanum tuberosum* cv. Désirée) were cultivated in sterile tissue culture in a phytochamber (16 h light, ~140 μE, 22 °C). Plants were transferred to steam-sterilized soil and grown for 4 weeks under long day conditions in a phytochamber (16 h light, ~140 μE, 60% humidity, 20 °C). PAMP treatment was performed with leaf disks that were cut out from 4-week-old potato plants with a biopsy puncher (4 mm diameter) and placed with the abaxial side onto the surface of 250 μl of water in a 96-well plate. The plate was incubated overnight at 22 °C in the dark. Water from the wells was removed and 100 μl sterilized fresh water per well was added. The plate was incubated for 30 min in the phytochamber (20 °C). Elicitation was performed by adding 100 nM StPIP1_1 (RLPSGSPRGPGRGH), Pep-13 (VWNQPVVRGFKVYE) or the nearly inactive analog W2A (VANQPVVRGFKVYE^{24, 27}). For whole plant assays, peptides were infiltrated as a 100 μM solution into the abaxial side of leaves of 3-week-old potato plants growing in a phytochamber. *Phytophthora infestans* infections were achieved by drop-inoculation of 10 μl of a zoospore suspension (1 × 10⁵ zoospores/ml) onto the abaxial leaf surface. Inoculated leaves were kept at 100% humidity for the duration of the experiment. As controls, water was pipetted onto the leaves⁴². *Nicotiana benthamiana* was grown from seeds in the greenhouse. Transient expression was performed with *Agrobacterium tumefaciens* containing binary vectors. Eleven-day-old Arabidopsis seedlings (Col-0 and *rlk7-2* (SALK_083114)) grown in microtiter plates were treated with 1 μM StPIP1_1.

RNA expression analyses

RNA was isolated from potato leaves, leaf disks or Arabidopsis seedlings as described²⁶. DNase digestion (RNase-free DNase Set, Qiagen) and cDNA synthesis using Maxima H Minus First Strand cDNA Synthesis Kit (Thermo Fisher Scientific) were performed according to the manufacturer's instructions. For quantitative PCR, Maxima Probe qPCR MasterMix (Thermo Fischer Scientific) was used and the samples were run on an Mx3005p qPCR system (Agilent).

The following primers and real time probes were used: *StPIP1_1*: 5'-GGAAATTCGTCTCGCAACTT-3', 5'-CTGAAGGTAGCCTCTCAAGCA-3' and Roche Universal Probe Library Probe #155, *StPRI*: 5'-TCAGTT CGACTAGGTTGTGGTC-3', 5'-GTCCGACCCAGTTTCCAAC-3' and probe #157, *St4CL*: 5'-TGCTGTTGT CCAATGATAGA-3', 5'-TGATCTAACAAACAAAAGCCACTG-3' and probe #7, *StTHT*: 5'-CCTCCTTAGAGG GCTTGCTT-3', 5'-AGTACGGATGGCCCGTAGA-3' and probe #144, *StRLK7*: 5'-TGGAAAGCCTAGAGAATG GTACA-3', 5'-CAAATGAAACGAGCACCACA-3' and probe #83, *StEF1α*: 5'-CACTGCCAGGTCATCATC-3', 5'-GTCGAGCACTGGTGCATATC-3' and Roche Universal Probe Library Probe #163, *AtFRK1*: 5'-GAGACT ATTTGGCAGGTA AAAAGGT-3', 5'-AGGAGGCTTACAACCATTGTG-3' and probe #33.

ROS assay

ROS analyses were performed as described⁴³ with the following modifications: Each well contained 200 µl of water supplied with 5 µM luminol L-012 (Wako Chemicals), 2 µg horseradish peroxidase (Fluka) and 100 nM peptide.

Liquid chromatography-mass spectrometry measurements

Leaf disks from 4-week-old infiltrated potato plants were cut out at defined time points after infiltration and frozen in liquid nitrogen. Chromatographic separations of methanolic extracts were performed as described previously^{44,45} with the following modifications of the binary gradient with 0.150 µl/min: 0–1 min isocratic 95% A (water/formic acid, 99.9/0.1 [v/v]) and 5% B (acetonitrile/formic acid, 99.9/0.1 [v/v]); 1–10 min linear from 5 to 60% B; 10–10.2 min linear to 95% B; 10.2–12 min isocratic 95% B; 12–14 min isocratic 5% B. Eluting compounds were detected from m/z 50 to 1000. LC-MS profiling data were analysed as described previously^{45,46}.

Infiltrated peptides of StPIP1_1 and Pep-13, which both had a carboxy-terminal amidation, were annotated by comparison of consistent retention time, accurate mass and MS/MS identity to the applied authentic standards. Deamidated peptides and peptide fragments were annotated by accurate mass as calculated from possible peptide structures generated in silico and by MS/MS sequence interpretation.

Subcellular localization of StPIP1_1-mCherry

A gene encompassing the coding region of StPIP1_1 fused to mCherry containing an intron was synthesized by GeneArt (ThermoFisher). The gene was cloned into a binary vector under the control of the 35S promoter by Golden Gate Cloning⁴⁷. As plasma membrane marker, Arabidopsis SULTR1;2 was included³³. The coding sequence of SULTR1;2 without the stop codon was amplified from Arabidopsis cDNA using the primers 5'-GGG GACAAGTTTGTACAAAAAAGCAGGCTTCATGTCGTCAGAGCTCACCTGTGG-3' and 5'-GGGGAC CACTTTGTACAAGAAAGCTGGGTCTCAGACCTCGTTGGAGAGTTTGG-3, cloned into pDONR221 via BP Ligation, and mobilized into pB7FWG2⁴⁸ to generate *ProCaMV35:SULTR1;2-GFP*. *Agrobacterium tumefaciens* GV3101 containing *StPIP1_1-mCh*, *SULTR1;2* or the silencing suppressor *p19* in a 1:1:2 ratio were co-infiltrated for transient expression in *N. benthamiana*. Three days after infiltration, microscopy was performed using a Zeiss LSM 780 inverted microscope using a 40× water-immersion objective. The excitation wavelengths for GFP and mCherry were 488 nm and 561 nm, respectively, and emission was detected between 495 and 550 nm (GFP) and 570 and 620 nm (RFP). Bright field images were captured with the TPMT detector. Plasmolysis was induced by application of 150 mM NaCl to excised leaf discs mounted on object slides.

Immunoblot analysis

Proteins were analyzed from *N. benthamiana* leaves expressing StPIP1_1-mCherry or ΔSP-StPIP1_1-mCherry 3 days after *Agrobacterium* infiltration. Leaves were ground in liquid nitrogen and the leaf material was mixed with 2× Laemmli buffer in a 1:1 ratio. For each sample, 20 µl were loaded on a 10% SDS gel and blotted for 1 h. Blots were blocked in 1× TBS with 2% [w/v] milk powder and 2% [w/v] BSA for 1 h at RT. For protein detection, blots were incubated over night at 4 °C with a primary mouse α-RFP antibody (1:1000; 6G6, Chromotek) and subsequently for 2 h at RT with a secondary α-mouse antibody coupled to horseradish peroxidase (1:20,000; A9044, Sigma-Aldrich). Western blot images were acquired with a FluorChem system detection using ECL-Prime (Amersham/Cytiva) for detection.

The authors confirm that all methods were carried out in accordance with the relevant guidelines.

Data availability

The datasets used and/or analysed during the current study available from the corresponding author on request.

Received: 7 June 2023; Accepted: 16 November 2023

Published online: 23 November 2023

References

- Choi, J. *et al.* Identification of a plant receptor for extracellular ATP. *Science* **343**, 290–294 (2014).
- Zhang, X. & Mou, Z. Extracellular pyridine nucleotides induce PR gene expression and disease resistance in Arabidopsis. *Plant J.* **57**, 302–312 (2009).
- Mazzoleni, S. *et al.* Inhibitory effects of extracellular self-DNA: A general biological process?. *New Phytol.* **206**, 127–132 (2015).
- Pearce, G., Strydom, D., Johnson, S. & Ryan, C. A. A polypeptide from tomato leaves induces wound-inducible proteinase inhibitor proteins. *Science* **253**, 895–897 (1991).
- Pearce, G., Moura, D. S., Stratmann, J. & Ryan, C. A. Jr. RALF, a 5-kDa ubiquitous polypeptide in plants, arrests root growth and development. *Proc. Natl. Acad. Sci. U.S.A.* **98**, 12843–12847 (2001).
- Huffaker, A., Pearce, G. & Ryan, C. A. An endogenous peptide signal in Arabidopsis activates components of the innate immune response. *Proc. Natl. Acad. Sci. U.S.A.* **103**, 10098–10103 (2006).
- Gully, K. *et al.* The SCOOP12 peptide regulates defense response and root elongation in *Arabidopsis thaliana*. *J. Exp. Bot.* **70**, 1349–1365 (2019).
- Hou, S. *et al.* The secreted peptide PIP1 amplifies immunity through receptor-like kinase 7. *PLoS Pathog.* **10**, e1004331 (2014).
- Luo, L. Plant cytokine or phyto cytokine. *Plant Signal. Behav.* **7**, 1513–1514 (2012).
- Gust, A. A., Pruitt, R. & Nürnberger, T. Sensing danger: Key to activating plant immunity. *Trends Plant Sci.* **22**, 779–791 (2017).
- Rzemieniewski, J. & Stegmann, M. Regulation of pattern-triggered immunity and growth by phyto cytokines. *Curr. Opin. Plant Biol.* **68**, 102230 (2022).
- Wang, L. *et al.* The systemin receptor SYR1 enhances resistance of tomato against herbivorous insects. *Nat. Plants* **4**, 152–156 (2018).
- Stegmann, M. *et al.* The receptor kinase FER is a RALF-regulated scaffold controlling plant immune signaling. *Science* **355**, 287–289 (2017).

14. Yamaguchi, Y., Pearce, G. & Ryan, C. A. The cell surface leucine-rich repeat receptor for AtPep1, an endogenous peptide elicitor in Arabidopsis, is functional in transgenic tobacco cells. *Proc. Natl. Acad. Sci. U.S.A.* **103**, 10104–10109 (2006).
15. Huffaker, A. & Ryan, C. A. Endogenous peptide defense signals in Arabidopsis differentially amplify signaling for the innate immune response. *Proc. Natl. Acad. Sci. U.S.A.* **104**, 10732–10736 (2007).
16. Ma, Y., Walker, R. K., Zhao, Y. & Berkowitz, G. A. Linking ligand perception by PEPR pattern recognition receptors to cytosolic Ca²⁺ elevation and downstream immune signaling in plants. *Proc. Natl. Acad. Sci. U.S.A.* **109**, 19852–19857 (2012).
17. Aalen, R. B., Wildhagen, M., Sto, I. M. & Butenko, M. A. IDA: A peptide ligand regulating cell separation processes in Arabidopsis. *J. Exp. Bot.* **64**, 5253–5261 (2013).
18. Guillou, M. C. *et al.* The *PROSCOOP10* gene encodes two extracellular hydroxylated peptides and impacts flowering time in Arabidopsis. *Plants* **11**, 3554 (2022).
19. Vie, A. K. *et al.* The IDA-LIKE peptides IDL6 and IDL7 are negative modulators of stress responses in *Arabidopsis thaliana*. *J. Exp. Bot.* **68**, 3557–3571 (2017).
20. Rhodes, J. *et al.* Perception of a divergent family of phytocytokines by the Arabidopsis receptor kinase MIK2. *Nat. Commun.* **12**, 705 (2021).
21. Zheng, X. *et al.* Danger-associated peptides close stomata by OST1-independent activation of anion channels in guard cells. *Plant Cell* **30**, 1132–1146 (2018).
22. Hou, S. G., Shen, H. X. & Shao, H. W. PAMP-induced peptide 1 cooperates with salicylic acid to regulate stomatal immunity in *Arabidopsis thaliana*. *Plant Signal. Behav.* **14**, 1666657 (2019).
23. Combest, M. M. *et al.* StPIP1, a PAMP-induced peptide in potato, elicits plant defenses and is associated with disease symptom severity in a compatible interaction with Potato virus Y. *J. Exp. Bot.* **72**, 4472–4488 (2021).
24. Brunner, F. *et al.* Pep-13, a plant defense-inducing pathogen-associated pattern from *Phytophthora* transglutaminases. *EMBO J.* **21**, 6681–6688 (2002).
25. Halim, V. A. *et al.* The oligopeptide elicitor Pep-13 induces salicylic acid-dependent and-independent defense reactions in potato. *Physiol. Mol. Plant Pathol.* **64**, 311–318 (2004).
26. Halim, V. A. *et al.* PAMP-induced defense responses in potato require both salicylic acid and jasmonic acid. *Plant J.* **57**, 230–242 (2009).
27. Nietzsche, L. *et al.* Early Pep-13-induced immune responses are SERK3A/B-dependent in potato. *Sci. Rep.* **9**, 18380 (2019).
28. Landgraf, R. *et al.* The ABC transporter ABCG1 is required for suberin formation in potato tuber periderm. *Plant Cell* **26**, 3403–3415 (2014).
29. Kloosterman, B. *et al.* Genes driving potato tuber initiation and growth: Identification based on transcriptional changes using the POCI array. *Funct. Integr. Genom.* **8**, 329–340 (2008).
30. Gamir, J. *et al.* The sterol-binding activity of PATHOGENESIS-RELATED PROTEIN 1 reveals the mode of action of an antimicrobial protein. *Plant J.* **89**, 502–509 (2017).
31. Schmidt, A. *et al.* Cloning and expression of a potato cDNA encoding hydroxycinnamoyl-CoA: tyramineN-(hydroxycinnamoyl) transferase. *J. Biol. Chem.* **274**, 4273–4280 (1999).
32. Schmidt, A., Scheel, D. & Strack, D. Elicitor-stimulated biosynthesis of hydroxycinnamoyltyramines in cell suspension cultures of *Solanum tuberosum*. *Planta* **205**, 51–55 (1998).
33. Takahashi, H. Sulfate transport systems in plants: Functional diversity and molecular mechanisms underlying regulatory coordination. *J. Exp. Bot.* **70**, 4075–4087 (2019).
34. Yasuda, S., Okada, K. & Saijo, Y. A look at plant immunity through the window of the multitasking coreceptor BAK1. *Curr. Opin. Plant Biol.* **38**, 10–18 (2017).
35. Campos, L. *et al.* Transgenic tomato plants overexpressing tyramine N-hydroxycinnamoyltransferase exhibit elevated hydroxycinnamic acid amide levels and enhanced resistance to *Pseudomonas syringae*. *Mol. Plant Microbe Interact.* **27**, 1159–1169 (2014).
36. Hander, T. *et al.* Damage on plants activates Ca²⁺-dependent metacaspases for release of immunomodulatory peptides. *Science* **363**, eaar7486 (2019).
37. Shen, W., Liu, J. & Li, J. F. Type-II metacaspases mediate the processing of plant elicitor peptides in Arabidopsis. *Mol. Plant* **12**, 1524–1533 (2019).
38. Butenko, M. A. *et al.* *INFLORESCENCE DEFICIENT IN ABSCISSION* controls floral organ abscission in Arabidopsis and identifies a novel family of putative ligands in plants. *Plant Cell* **15**, 2296–2307 (2003).
39. Scharon, K. *et al.* Precursor processing for plant peptide hormone maturation by subtilisin-like serine proteinases. *Science* **354**, 1594–1597 (2016).
40. Ziemann, S. *et al.* An apoplastic peptide activates salicylic acid signalling in maize. *Nat. Plants* **4**, 172–180 (2018).
41. Shen, J. *et al.* Secreted peptide PIP1 induces stomatal closure by activation of guard cell anion channels in Arabidopsis. *Front. Plant Sci.* **11**, 1029 (2020).
42. Eschen-Lippold, L. *et al.* Reduction of divinyl ether-containing polyunsaturated fatty acids in transgenic potato plants. *Phytochemistry* **68**, 797–801 (2007).
43. Trujillo, M. Analysis of the immunity-related oxidative bursts by a luminol-based assay. *Methods Mol. Biol.* **1398**, 323–329 (2016).
44. Böttcher, C. *et al.* Metabolome analysis of biosynthetic mutants reveals a diversity of metabolic changes and allows identification of a large number of new compounds in Arabidopsis. *Plant Physiol.* **147**, 2107–2120 (2008).
45. Gorzalka, K., Perino, E. H. B., Lederer, S., Smolka, U. & Rosahl, S. Lysophosphatidylcholine 17:1 from the leaf surface of the wild potato species *Solanum bulbocastanum* inhibits *Phytophthora infestans*. *J. Agric. Food Chem.* **69**, 5607–5617 (2021).
46. Dobritsch, M. *et al.* MATE transporter-dependent export of hydroxycinnamic acid amides. *Plant Cell* **28**, 583–596 (2016).
47. Engler, C. *et al.* A golden gate modular cloning toolbox for plants. *ACS Synth. Biol.* **3**, 839–843 (2014).
48. Karimi, M., Inze, D. & Depicker, A. GATEWAY vectors for Agrobacterium-mediated plant transformation. *Trends Plant Sci.* **7**, 193–195 (2002).

Acknowledgements

We thank Dierk Scheel and Tina Romeis (IPB Halle) for support and Philip Weckwerth (IPB Halle) for helpful discussions and critical reading of the manuscript. This work was funded by the German Research Foundation SFB 648, TP A4.

Author contributions

L.N., U.S., E.H. B.P., K.G., G.S. performed experiments, S.M., K.B., S.R. designed the research, S.R. wrote the manuscript.

Funding

Open Access funding enabled and organized by Projekt DEAL.

Competing interests

The authors declare no competing interests.

Additional information

Supplementary Information The online version contains supplementary material available at <https://doi.org/10.1038/s41598-023-47648-x>.

Correspondence and requests for materials should be addressed to S.R.

Reprints and permissions information is available at www.nature.com/reprints.

Publisher's note Springer Nature remains neutral with regard to jurisdictional claims in published maps and institutional affiliations.



Open Access This article is licensed under a Creative Commons Attribution 4.0 International License, which permits use, sharing, adaptation, distribution and reproduction in any medium or format, as long as you give appropriate credit to the original author(s) and the source, provide a link to the Creative Commons licence, and indicate if changes were made. The images or other third party material in this article are included in the article's Creative Commons licence, unless indicated otherwise in a credit line to the material. If material is not included in the article's Creative Commons licence and your intended use is not permitted by statutory regulation or exceeds the permitted use, you will need to obtain permission directly from the copyright holder. To view a copy of this licence, visit <http://creativecommons.org/licenses/by/4.0/>.

© The Author(s) 2023